

Supporting information

Enhanced Operational Stability through Interfacial Modification by Active Encapsulation of Perovskite Solar Cells

Sudeshna Ghosh¹, Roja Singh², Anand S. Subbiah², Pablo P. Boix³, Ivan Mora-Sero⁴ and Shaibal K Sarkar²

¹ Center of Research in Nanotechnology and Science, Powai, Mumbai 400 076 India

² Department of Energy Science and Engineering, Indian Institute of Technology Bombay, Powai, Mumbai 400 076 India

³ Institut de Ciència dels Materials, University of Valencia Catedràtic J. Beltran 246980 Paterna, Valencia, Spain

⁴ Institute of Advanced Materials, Universitat Jaume I, Av. de Vicent Sos Baynat, s/n 12071 Castelló de la Plana, Spain

Corresponding Author

shaibal.sarkar@iitb.ac.in.

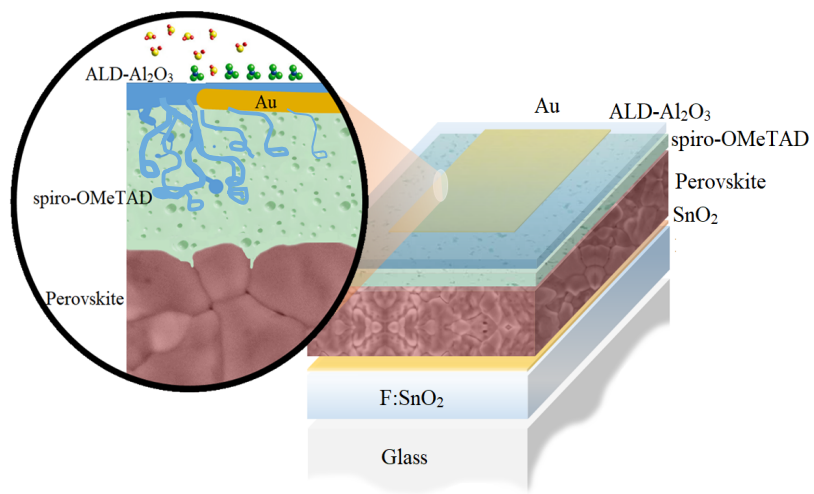


FIG. S1. Schematic of Triple cation mixed halide based perovskite devices with 30nm ALD- Al_2O_3 on top of gold act as encapsulant.

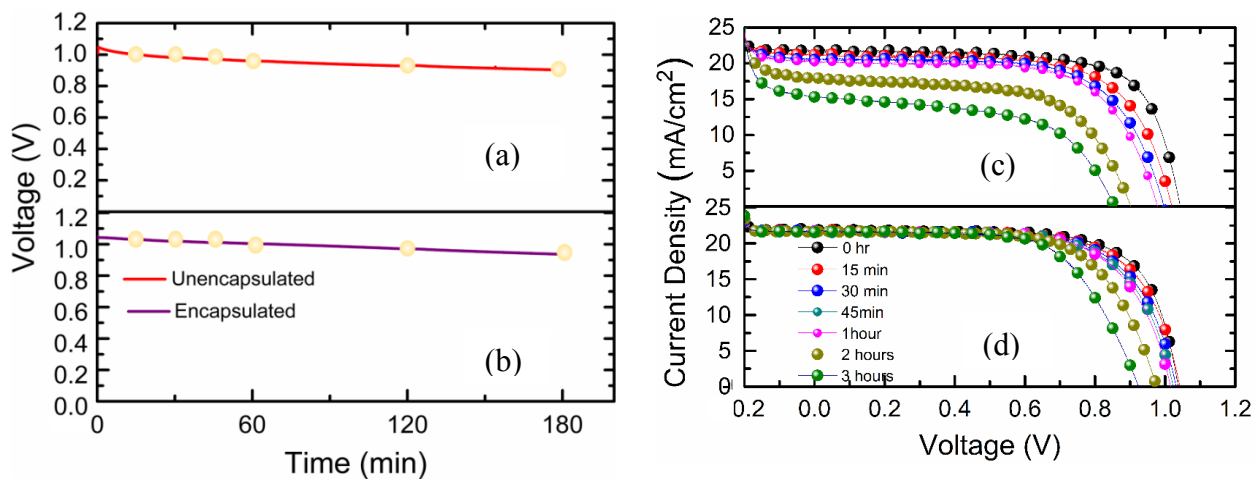


FIG. S2. V_{oc} vs time for (a) unencapsulated and (b) encapsulated devices along with intermittent J-V (forward direction) for (c) unencapsulated and (d) encapsulated devices measured at 0min, 15 min, 30 min, 60 min, 120 min and 180 min. In Figure (a) and (b) no reduction in voltage is visible in both devices. Along with V_{oc} vs time intermittent light J-V of unencapsulated devices show a visible decrement of FillFactor (FF) compared to encapsulated devices.

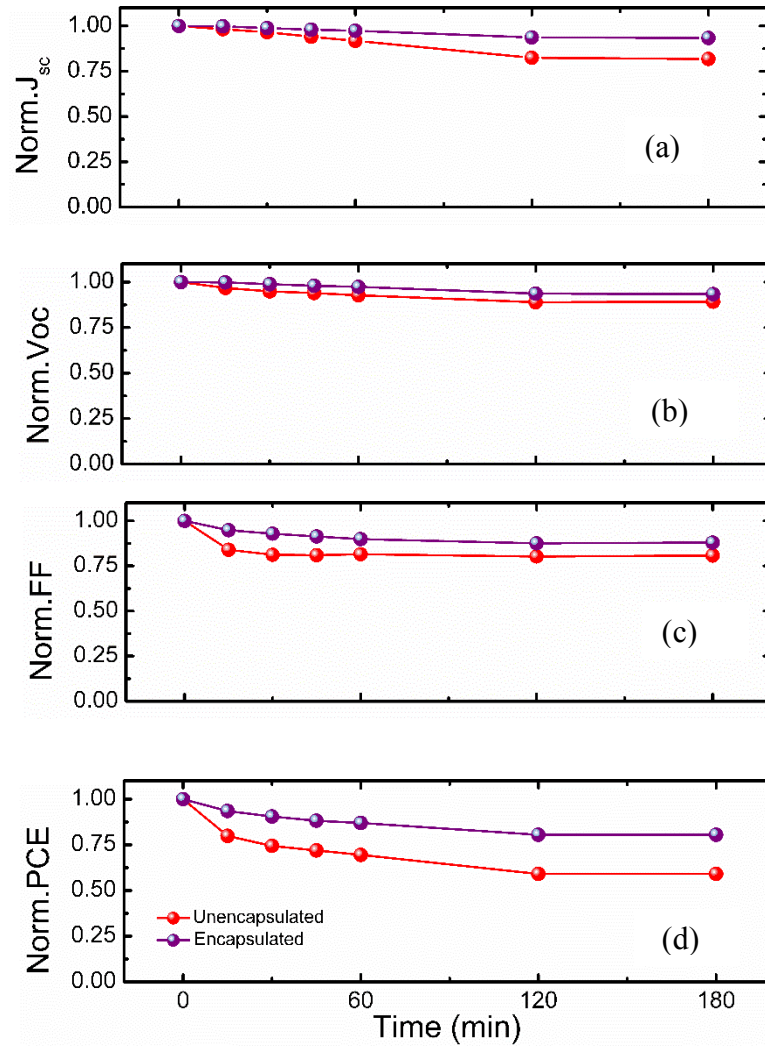


FIG. S3. Variation of normalized different parameters with time of unencapsulated and encapsulated devices for 0 min,15 min,30 min,45 min,60 min,120 min,180 min where (a) J_{sc} vs t (b) V_{oc} vs t (c) FF vs t (d) PCE vs t extracted from intermittent J-V . There is very less change in V_{oc} with time in both the devices depicting that bulk properties are unchanged during the measurement .On the other hand, during intermittent J vs V, FF of unencapsulated devices are significantly affected causing efficiency lower while in encapsulated devices comparatively less change in FF resulting encapsulated devices more stable.

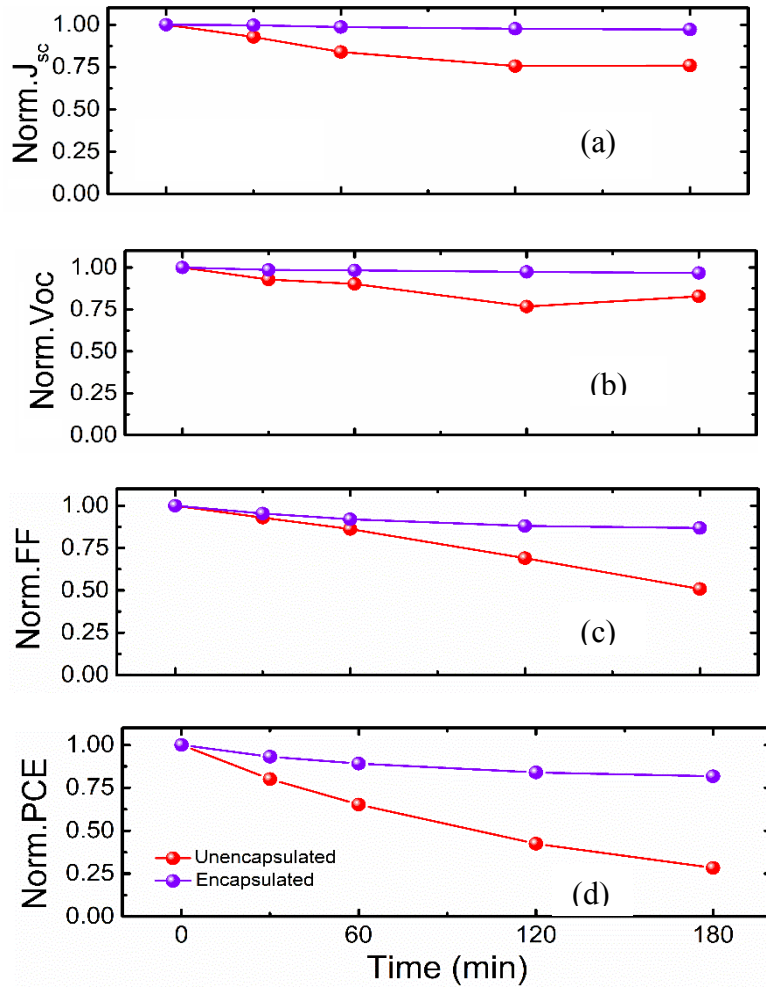


FIG. S4. Variation of normalized different parameters (a) J_{sc} (b) V_{oc} (c) FillFactor (FF) (d) PCE with time for 0min,30min,60min,120min,180 min of unencapsulated and encapsulated devices extracted from J_{sc} vs t with intermittent J vs V measurement. In unencapsulated devices, drastic decrease in J_{sc} , V_{oc} and FF causing decrease in efficiency drastically whereas in encapsulated devices slight decrease in FF cause slight change in efficiency.

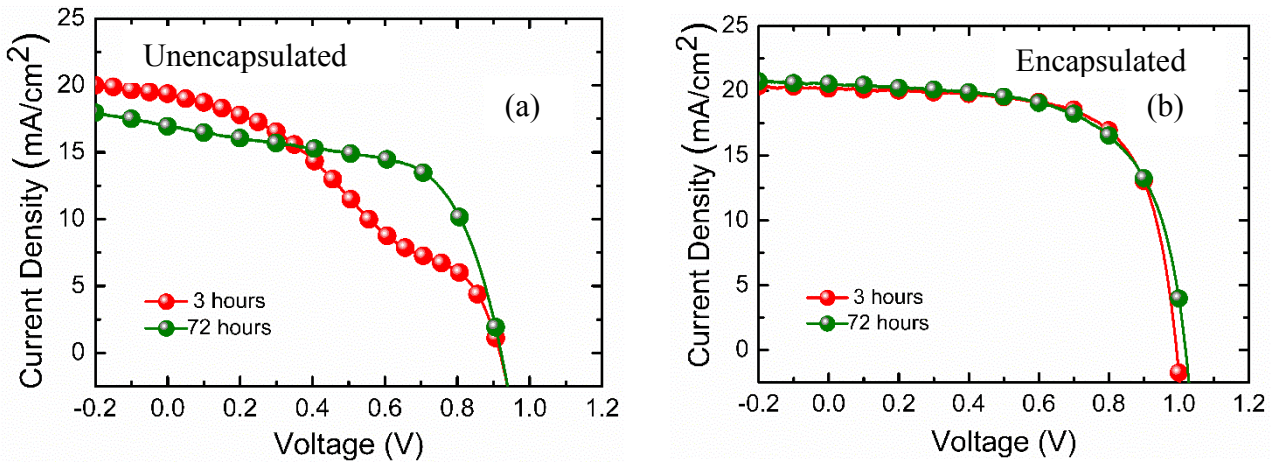


FIG. S5. Dark recovery of J-V characteristics (a) unencapsulated devices (b) encapsulated devices with measurement after 3 hours (red) and 72 hours dark recovery (green). S kink feature disappeared in unencapsulated devices after 72 hours dark recovery whereas encapsulated devices slight increase in V_{oc} after dark recovery.

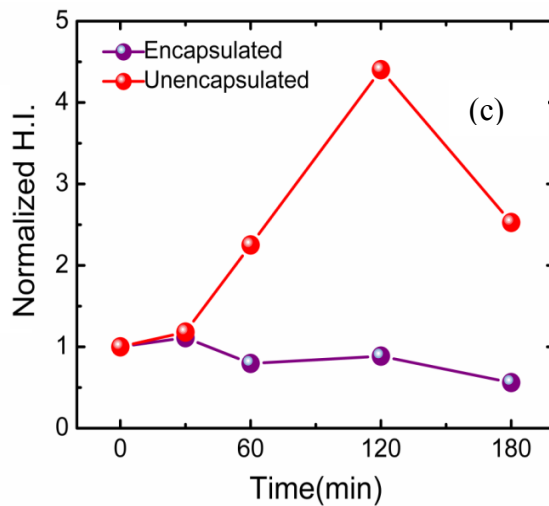
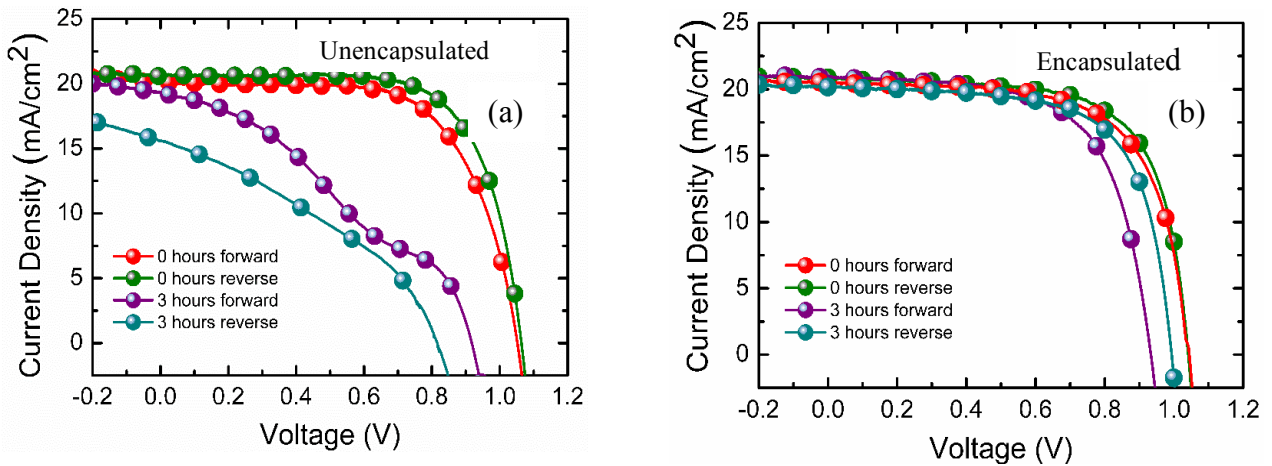


FIG. S6. Forward (FS) and Reverse scan (RS) of (a) unencapsulated and (b) encapsulated devices where FS (red) and RS (green) for 0 hours, and FS (violet) and RS (cyan blue) after 3 hours (c) Variation of hysteresis index with time in the case of unencapsulated devices (red) and encapsulated devices (purple). Inverted hysteresis is observed in unencapsulated devices along with larger hysteresis index compared to encapsulated devices as shown in Figures (a), (b) and (c).

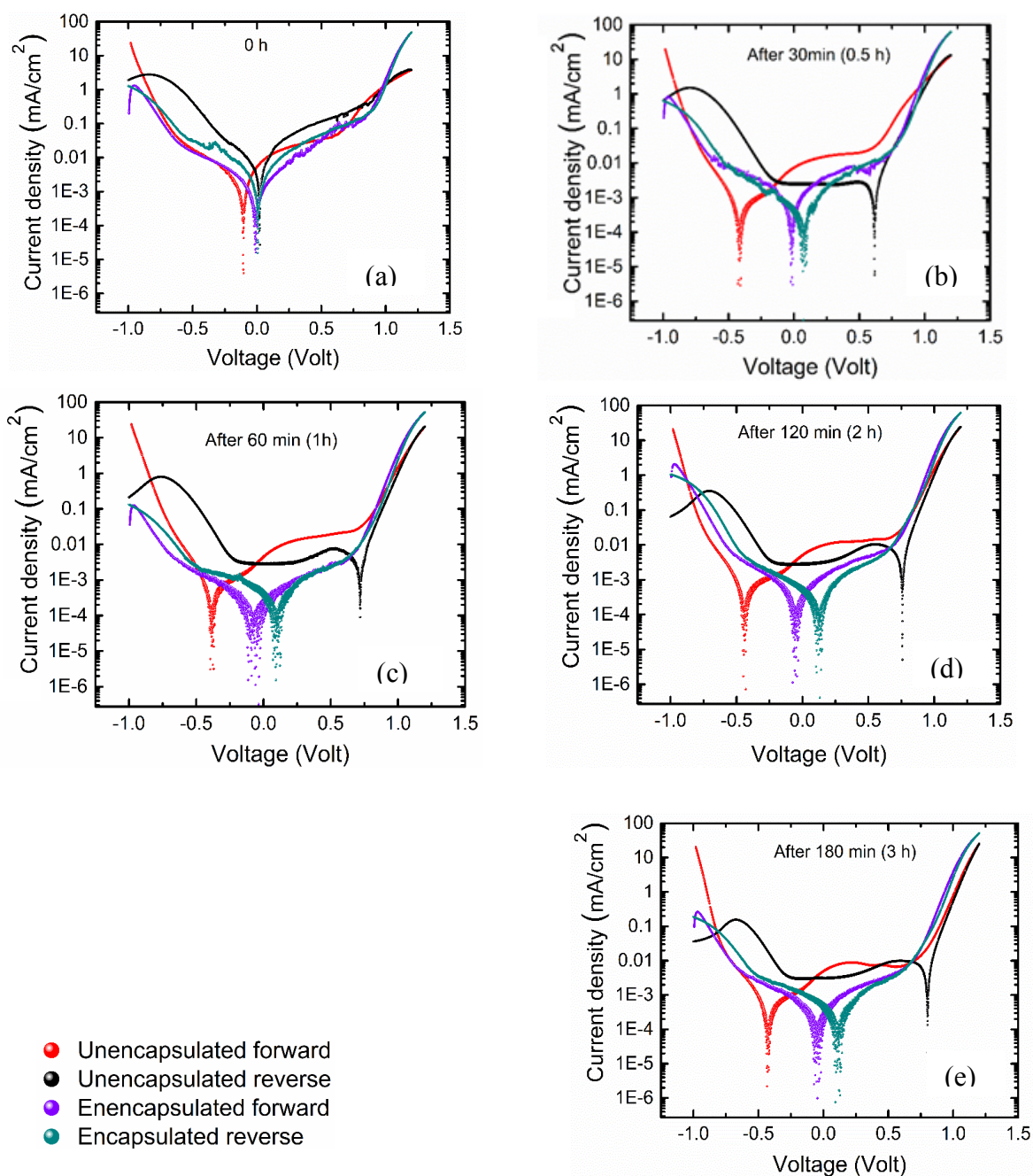


FIG. S7. Dark J-V curve for unencapsulated and encapsulated devices in semi-logarithmic scale where Figure (a) represents initial condition where the crossover point is close to 0 Volt in both the devices representing absence of slow phenomena. Figure (b) represent the dark J-V after 30 min chronoamperometry (J_{sc} vs t). In this case (30 min), we can see that in unencapsulated devices the cross over points are widely separated whereas in encapsulated devices it is almost coinciding means prominent signature of some slow phenomena in unencapsulated devices whereas in encapsulated devices no such slow phenomena is present. Figures (c), (d), (e) representing the dark J-V after 60min, 120 min, 180min chronoamperometry (J_{sc} vs t) measurement where the crossover points in unencapsulated devices are departed from each other more as measurement time increases. As the time increases, presence of more and more slow phenomena observed in unencapsulated devices whereas it is absent in encapsulated one.

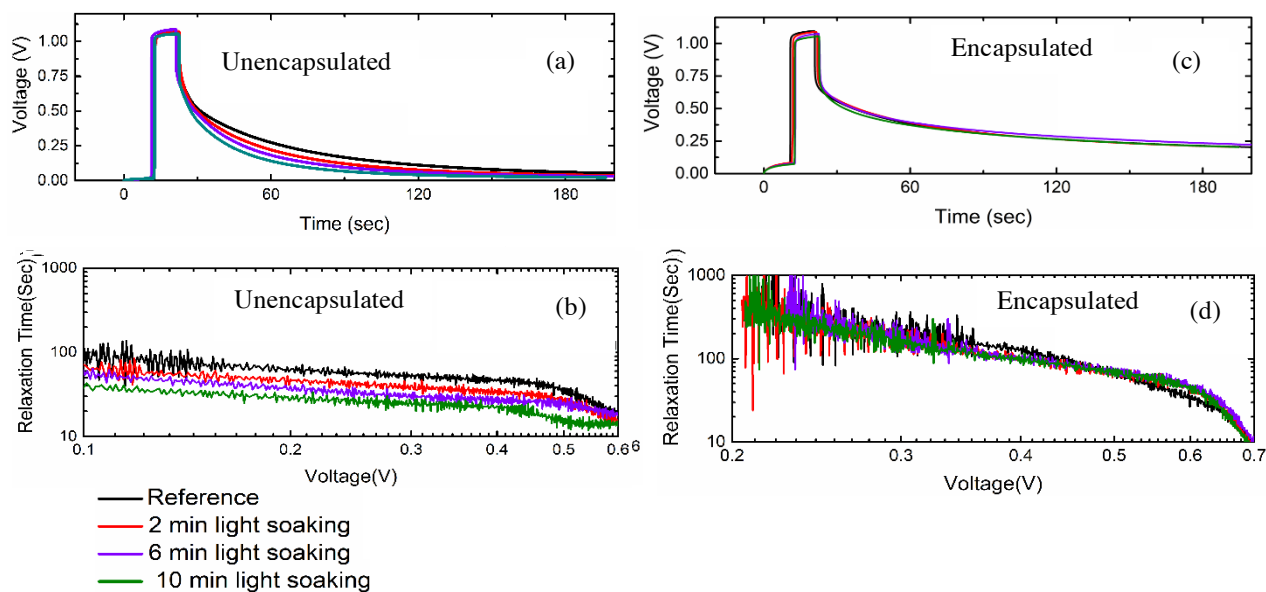


FIG. S8. Open Circuit Voltage Decay under different light soaking condition for (a) unencapsulated and (c) encapsulated devices [reference(black),2 min (red),6 min(violet),10 min (green) light soaking]. In Figure (a) for unencapsulated devices the decay properties are changing with light soaking duration whereas in encapsulated devices, no such effects are observed as shown in Figure (c). Variation of Relaxation time vs. voltage of unencapsulated and encapsulated devices in Figure (b) and (d) under different light soaking duration [reference (black),2min (red),6 min(violet),10 min(green) light soaking]. In Figure (b)for unencapsulated devices the decay properties are changing with light soaking duration whereas in encapsulated devices as shown in Figure (d), no such effects are observed.

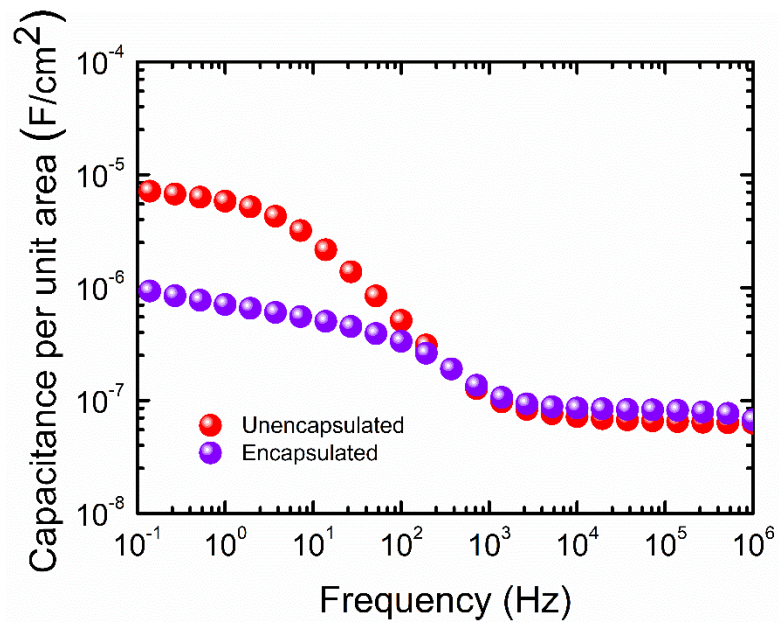


FIG. S9. Variation of low frequency (LF) Capacitance per unit area vs. frequency under dark at 0 V condition of unencapsulated (red) and encapsulated (violet) devices where we can see the LF capacitance per unit area of unencapsulated device is of the order of 10^{-5} F/cm² and the capacitance per unit area of encapsulated device is of the order of 10^{-6} F/cm². The low frequency capacitance per unit area of unencapsulated device is one order higher compared to encapsulated device.

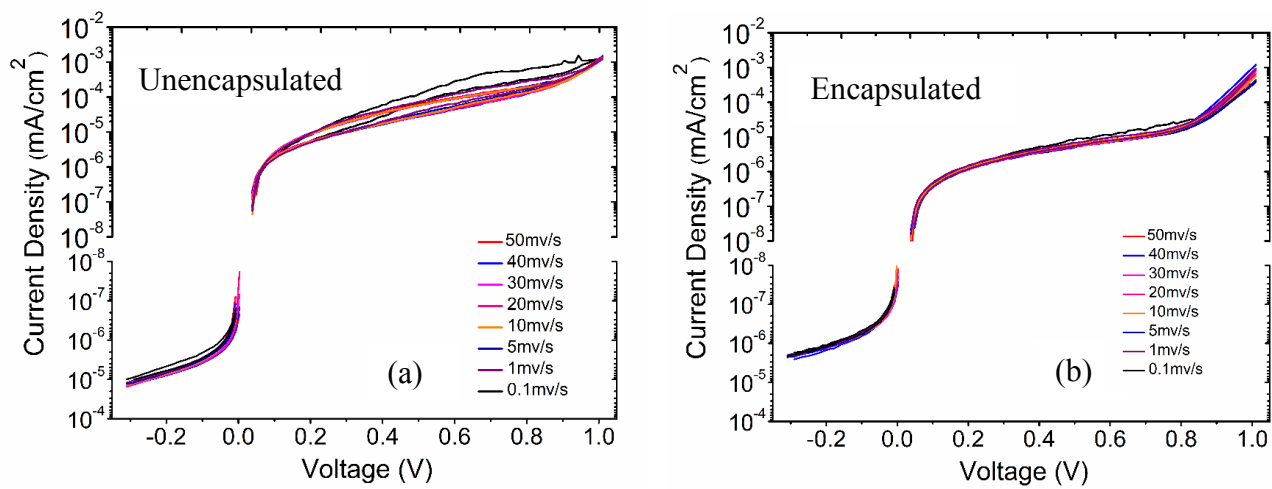


FIG. S10. Dark Capacitive Current Density of (a) unencapsulated and (b) encapsulated devices at varying scan rate.

The dark J-V measured at different scan rates from 50 mV/s to 0.1 mv/s .Then it is plotted in the semilogarithmic scale to find out the capacitive and non-capacitive effect . As mentioned in Almora et. al, general form of the dark current can be categorized as below

$$J = J_0 \left[\exp \left(\frac{qV}{nk_B T} \right) - 1 \right] + \frac{V}{R_{sh}} + J_{cap} + J_{noncap} \quad (1)$$

The first term is the dark diode equation with J_0 as dark saturation current, q is the elementary charge, V is the applied voltage, k_B is the Boltzmann's constant and T is the temperature.

The second term is the leakage current with shunt resistance R_{sh} .

The capacitive current density J_{cap} for the other scan rates.can be calculated from the below equations

$$J_{cap} = J - J_{avg} \quad (2)$$

$$J_{cap} = \frac{dQ}{dt} = C \frac{dV}{dt} = C \cdot s \quad (3)$$

where, J is the average current density of forward and reverse sweep of the different scan rate. t is time, s is the scan rate.

Non capacitive current can be explained as:

$$J_{noncap} = J_{max} \left[1 + \exp \left(-\frac{q(V-V_0)}{nk_B T} \right) \right]^{-1} \quad (4)$$

The voltage V_0 is related to a reaction potential and q is charge, and V is applied potential .

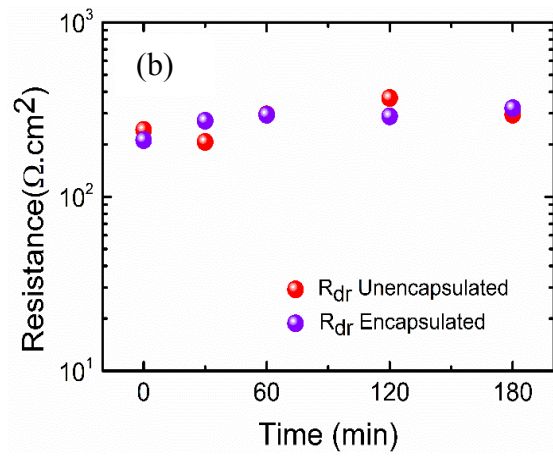
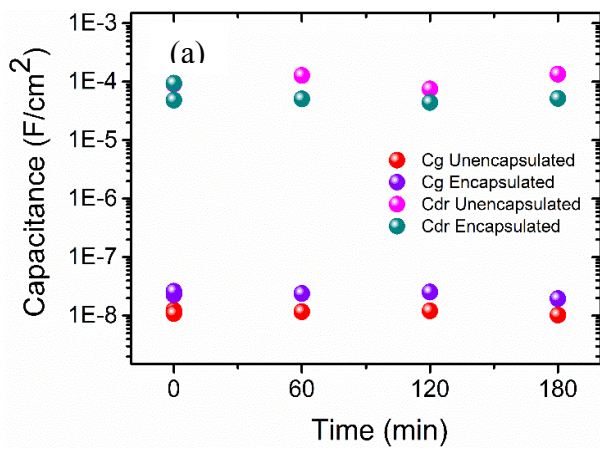


FIG. S11.(a) Variation in C_g (geometrical capacitance) and C_{dr} (dielectric capacitance) in unencapsulated (red) and encapsulated (violet) devices (b) Variation in R_{dr} (dielectric resistance) in unencapsulated and encapsulated devices calculated by fitting circuit. The value of C_g geometrical capacitance and C_{dr} dielectric capacitance are almost same of unencapsulated and encapsulated devices. The R_{dr} (dielectric resistance) value are almost same for both the devices.

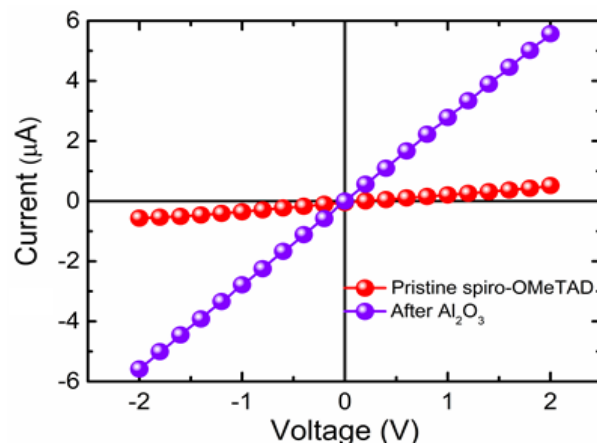
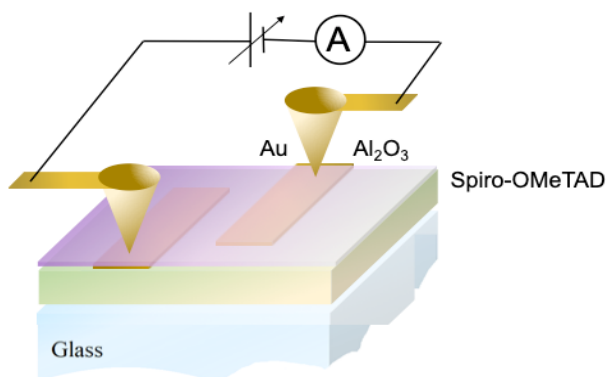


FIG. S12. spiro-OMeTAD conductivity before deposition (red) and after deposition of Al₂O₃ (violet). Hence we can see that one order enhancement of spiro-OMeTAD conductivity after Al₂O₃ deposition.

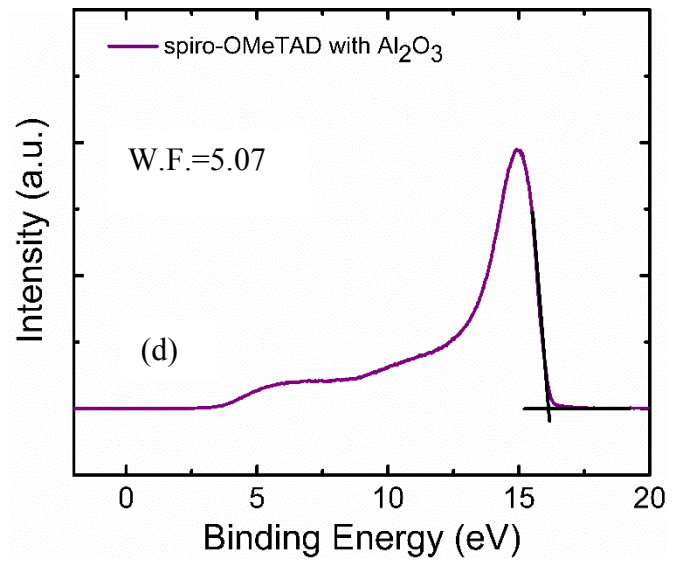
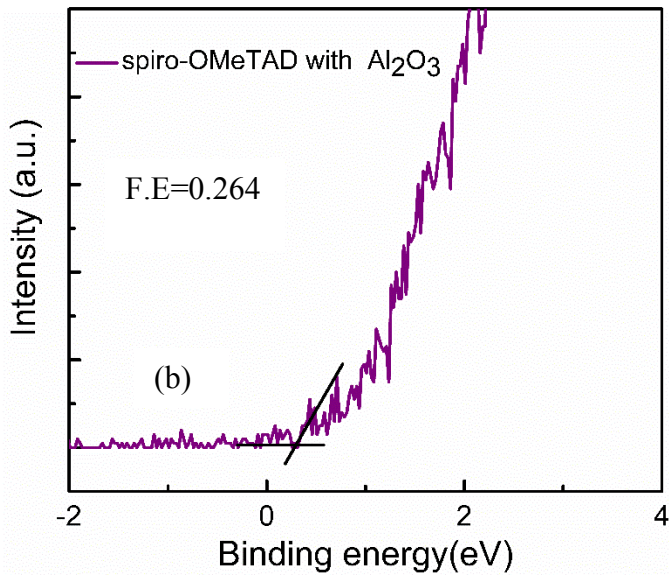
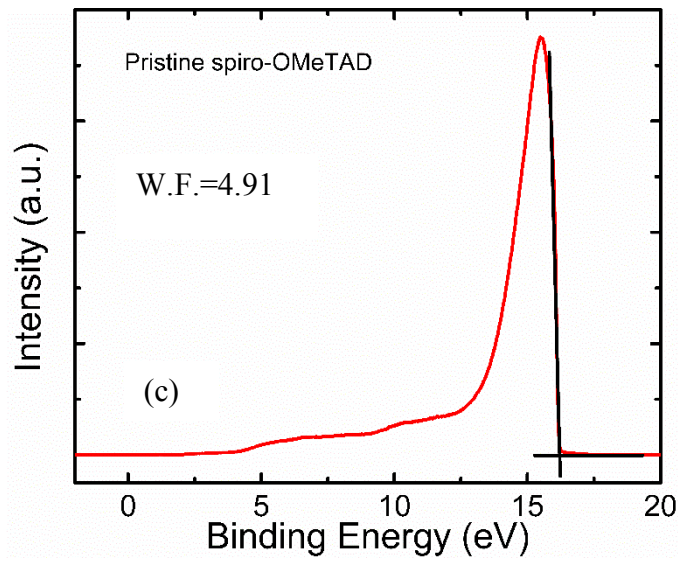
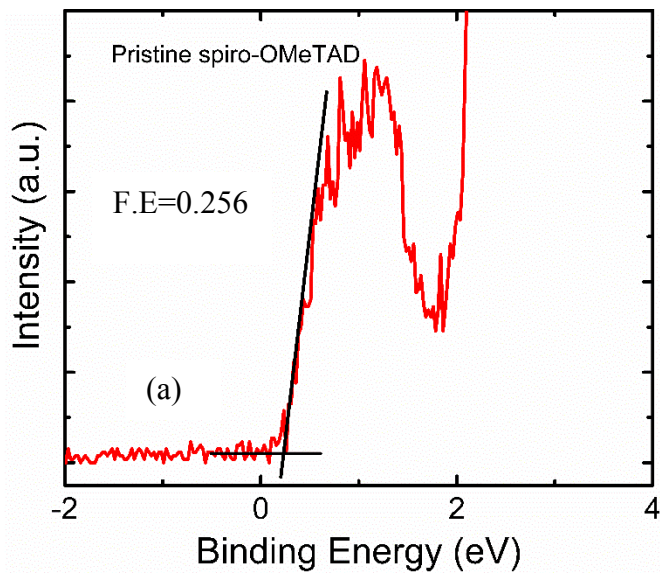


FIG. S13. UPS spectra of unencapsulated (a) and (b) and encapsulated devices (c) and (d) presenting Work function, Fermi-energy edge from Valance Band Minima (VBM). Work function in the case of spiro-OMeTAD with Al_2O_3 is increased by an amount of 0.16 eV compared to pristine spiro-OMeTAD.

Experimental section

FTO substrate preparation: F:SnO₂ (FTO, Tech-8) sheets were bought from Dyesol. The 3x3 FTO substrates are etched with Zn powder (Merck) and 2M HCl (Rankem) acid. The FTO substrates are then cleaned with alconox water solution followed by de-ionized water, acetone and iso-propanol solvents, for 10 min each. After cleaning with different solvents, the FTO substrates were dried and exposed to UV-treatment for 30 minutes.

SnO₂ ETL deposition: The 30 nm bi-layer SnO₂ as ETL was deposited on FTO substrates using spin coating method. The initial layer of SnO₂ solution was prepared by dissolving tin (IV) chloride pentahydrate (SnCl₄.5H₂O - 98%, Sigma Aldrich) in anhydrous iso-propanol (99.5 %, Sigma Aldrich) to accomplish 0.05 M concentration and spin coated on FTO substrates at 2000 rpm for 45 seconds. The substrates were then annealed at 180°C for 45 minutes. The SnO₂ films are again spin coated with SnO₂ colloidal dispersion, diluted (15% in H₂O colloidal dispersion, Alfa Aesar) in de-ionized water with the volume ratio 1:4 at 4000 rpm for 45 seconds. The substrates were again annealed at 150°C for 30 minutes to form bilayer SnO₂.

((FA)_{0.83}(MA)_{0.17})_{0.95}Cs_{0.05}PbI_{2.5}Br_{0.5} Perovskite absorber fabrication: The triple cation mixed halide perovskite absorber, ((FA)_{0.83}(MA)_{0.17})_{0.95}Cs_{0.05}PbI_{2.5}Br_{0.5} was prepared by using 1M formamidine hydroiodide (FAI), (low water content, Tokyo Chemical Industries), 0.2M methylamine hydrobromide (MABr), (low water content, Tokyo Chemical Industries), 1.1 M lead iodide (PbI₂), (99.9%, Tokyo Chemical Industries), 0.2M PbBr₂ lead bromide (PbBr₂), (99.9%, Tokyo Chemical Industries) dissolved in di-methylformamide (DMF), (anhydrous, 99.8%, Sigma Aldrich), dimethyl sulfoxide (DMSO), (anhydrous, 99.9%, Sigma Aldrich) 4:1 volume ratio followed by stirring. Later, 52 μ l solution from stock solution containing 1.5 M cesium iodide (CsI), (99.999%, Tokyo Chemical Industries) prepared in DMSO solvent was mixed with 1 ml of the previous precursor solution.³ The perovskite solution was spin-coated onto the UV -ozone treated SnO₂ coated FTO substrates using anti-solvent assisted spin-coating process at 2000 and 6000 rpm for 10 sec and 30 sec respectively. A 500 μ l of chlorobenzene (anhydrous, 99.8%, Sigma Aldrich) antisolvent was dripped on spinning substrates 15 sec

before the end of 30 sec spinning program for fast crystallization and then annealed at 100 °C for 30 minutes in nitrogen atmosphere inside a glove box.

Spiro-OMeTAD HTL deposition: 80 mg of spiro-OMeTAD (Luminescence Technology) was prepared in 1 ml chlorobenzene followed by subsequent addition of 24 μ l of 26 mg bis (trifluoromethane) sulfonamide lithium salt (Sigma Aldrich) dissolved in acetonitrile (anhydrous, 99.8%, Sigma Aldrich) and 40 μ l of 4-tert-butylpyridine (Sigma Aldrich). An 80 μ l of spiro-OMeTAD solution was spin coated dynamically at 4000rpm for 45 sec and left overnight for oxidation in ambient condition to enhance the conductivity of spiro-OMeTAD

Gold Metal Contact: Further, 80 nm gold metal (99.999%, Parekh Industries) is thermally evaporated inside a vacuum chamber with a base pressure 5×10^{-6} mbar to make contacts. To achieve active area of the devices of approximately 0.1 cm², a shadow mask is used

Al₂O₃ (ALD) Encapsulant deposition:

Encapsulant aluminium oxide (Al₂O₃) were deposited on top of devices with help of custom-built viscous flow hot wall reactor configuration at 75°C. The precursors are Trimethyl aluminium (TMA, from Gelest, Inc) and HPLC grade H₂O (from Sigma Aldrich, USA).⁴ All the reactants are used as received without any further purification and were always stored at room temperature. The carrier gas used during this deposition is nitrogen (N₂, 99.999%). The in depth discussion of reactor is given elsewhere.⁵

The precursor pulsing arrangement of (n-t₁-m-t₂) was used here, where ‘n’ and ‘m’ are the number of pulses of TMA and H₂O while ‘t₁’ and ‘t₂’ are the purge times after TMA and H₂O in seconds respectively. The constant dose times of 1 sec were maintained for both the reactants throughout the investigation. The transient pressure changes of ca. 0.1±0.05 Torr and 0.8±0.05 Torr were maintained during the TMA and H₂O exposures of 1 sec respectively and were continuously noticed with the help of capacitance manometer (MKS).

Characterization:

Current Voltage measurement (I-V measurement) was performed by using illuminator of Abet (Class A) Xenon lamp with KG-5 Filter, and gold-coated probe from Holmarc. The light-intensity was calibrated with help of silicon reference cells from Newport. A non – reflective light aperture of 3.14 mm² was used to describe active area and SP-150 potentiostat was used as source meter to measure the I-V characteristics.

Electro-chemical impedance spectroscopy (EIS) was done with the help of Metrohm - Autolab and the spectra were analyzed using Nova software. Dark I-V was also measured in the same system.

Open Circuit Voltage Decay (OCVD) was measured in Wave labs Sinus 70 solar simulator with self-calibrating setup. An illumination mask of 3.14 mm² was used for the same.

Ultraviolet Photoemission Spectroscopy (UPS) studies was conducted in Kratos analytical-AXIS Supra system using a high photon flux He gas discharge lamp (He-I 21.2 eV and He-II at 40.8 eV).

Experimental procedure

Photocurrent density vs time along with intermittent J-V and impedance measurement

The details of experimental procedures as follows-

Here, we have measured photocurrent density vs time for three hours along with intermittent J-V under dark and light condition and also the impedance under the same condition . At 0 min ,first the device is kept under light to define the active area followed by measuring J-V to ensure the devices initial performance .Then the devices are kept under dark in relaxed condition so that its voltage reduced and then dark J-V in both direction is measured to ensure its diode characteristics .After that,we have turned on light to measure

the light J-V in both direction followed by photo-chronoamperometry for 30 minutes. Further photo-chronoamperometry completing we have switched off the light and waited till the voltage get reduced .After that we measured dark J-V again to see the effect of light and bias and measured impedance under dark at 0 V condition to measure low frequency capacitance .After that we have switched on the light to measure impedance under light at Voc condition followed by light J-V. The same steps are repeated in the case of 1 hour (60 min),2 hours (120 min) ,3 hours (180 min).Here every step has its own scientific aspects .The light J-V before starting the photocurrent density vs voltage gives us the opportunity to know different parameters and then photochronoamperometry measurement under light gives us the opportunity to know effect of charge accumulation across the interfaces because of ionic contribution and the existence of barrier if any.The dark J-V measurement gives us the opportunity to know the effect of slow contribution if any present under the effect of bias,light.Then the impedance measurement under dark at 0V condition gives us the opportunity to know about low frequency capacitance that gives us the knowledge of electrode polarization effect and under light at Voc condition gives us the chance of seeing the effect of light, bias on different interfacial and bulk properties .Finally the light J-V measurement after all the steps gives us the chance to find out the most affected parameter because of change in interfacial and bulk condition if presence any.

Open circuit voltage decay (OCVD) measurement

In open circuit voltage decay

We have kept devices for 2 minutes,6 minutes,10 minutes for light soaking under 1 sun illumination and then switched off followed by a light pulse of 20 sec is given to rise the photovoltage .Further light is turned off and we measured the photovoltage decay of both the unencapsulated and encapsulated devices.

Capacitive and non-capacitive current measurement

The dark J-V measured at different scan rates from 50 mV/s to 0.1 mV/s .Then it is plotted in the semilogarithmic scale to find out the capacitive and non-capacitive effect .

Spiro-OMeTAD conductivity measurement

We measure conductivity of spiro-OMeTAD by making a film on glass where *spiro* – OMeTAD film is spin-coated and an inter-digited mask is used to make contacts on it .Another film of spiro-OMeTAD with Al₂O₃, where 30 nm ALD Al₂O₃ was deposited on top of gold inter-digited contacts. We measure the conductivity from the I-V of spiro –OMeTAD which follows

$$V = IR \quad (5)$$

Where V is the voltage and I is the current and R is the resistance .

Again ,

$$R = \frac{\rho l}{A} \quad (6)$$

$$\rho = \frac{RA}{l} \quad (7)$$

Where ρ is resistivity and l is the length and A is the active area

Now,
$$\sigma = \frac{1}{\rho} \quad (8)$$

Where σ is the conductivity of the film

¹ O. Almora, C. Aranda, I. Zarazua, A. Guerrero, and G. Garcia-Belmonte, ACS Energy Lett. **1**, 209 (2016).

² S.-M. Yoo, S.J. Yoon, J.A. Anta, H.J. Lee, P.P. Boix, and I. Mora-Seró, Joule **3**, 2535 (2019).

³ M. Saliba, T. Matsui, J.-Y. Seo, K. Domanski, J.-P. Correa-Baena, M.K. Nazeeruddin, S.M. Zakeeruddin, W. Tress, A. Abate, A. Hagfeldt, and M. Grätzel, Energy Environ. Sci. **9**, 1989 (2016).

⁴ M. D. Groner, F. H. Fabreguette, J. W. Elam, and S. M. George, Chem. Mater. **16**, 639 (2004).

⁵ N. Mahuli and S.K. Sarkar, J. Vac. Sci. Technol. A Vacuum, Surfaces, Film. **34**, 01A142 (2016).